Thermal Conductivity Models for Single and Multiple Filler Carbon/Liquid Crystal Polymer Composites

Rebecca A. Hauser, Jason M. Keith, Julia A. King, Jennifer L. Holdren

Department of Chemical Engineering, Michigan Technological University, Houghton, Michigan 49931-1295

Received 27 February 2008; accepted 24 June 2008
DOI 10.1002/app.28869
Published online 2 September 2008 in Wiley InterScience (www.interscience.wiley.com).

ABSTRACT: In this study, two different carbon fillers (Thermocarb TC-300 synthetic graphite and Fortafil 243 carbon fiber) were added to Vectra A950RX liquid crystal polymer to produce single filler composites with filler concentrations of up to 80 wt % (71.4 vol %) and multiple filler composites that contained varying concentrations of both synthetic graphite and carbon fiber. The through-plane and in-plane thermal conductivity for each formulation was measured. For the single filler synthetic graphite and carbon fiber composites, the Nielsen model was applied to the experimental through-plane thermal conductivity data. The parameters obtained from the single filler models were then used along with a variation of the original Nielsen model to predict the through-plane thermal conductivities of the multiple filler composites. In-plane thermal conductivity models were also developed using a correlation involving the square root of the product of the composite in-plane and through-plane thermal conductivities. This model was applied to the single filler synthetic graphite and carbon fiber composites. A variation of this model was then used to predict the in-plane thermal conductivity for composites containing both fillers. All the models presented in this work showed good agreement with experimental data. © 2008 Wiley Periodicals, Inc. J Appl Polym Sci 110: 2914–2923, 2008

Key words: composites; fillers; liquid-crystalline polymers (LCP); thermal properties

INTRODUCTION

Most polymer resins are thermally insulating. One emerging market for thermally conductive resins is for bipolar plates for use in fuel cells. The bipolar plate separates one cell from the next, with this plate carrying hydrogen gas on one side and air (oxygen) on the other side. Hydrogen reacts with oxygen from the air to produce DC electricity. Byproducts of the reaction are heat and water. Bipolar plates require high thermal conductivity (to conduct away the generated heat), low gas permeability, and good dimensional stability.

Typical thermal conductivity values in W/m K for some common materials are 0.2–0.3 for polymers, 234 for aluminum, 400 for copper, and 600 for graphite. One approach to improve the thermal conductivity of a polymer is through the addition of a conductive filler material, such as carbon and metal.[1–14] In a polymer containing conductive fillers, heat is transferred by two mechanisms, lattice vibrations (major contributor) and electron movement.[2] Typically, a single type of carbon is used in thermosetting resins (often a vinyl ester) to produce a thermally conductive bipolar plate material with a desired thermal conductivity of at least 20 W/m K.[15–18] Thermosetting resins cannot be remelted.

In this work, researchers performed compounding runs followed by injection molding and thermal conductivity testing of carbon/Vectra A950RX composites. Vectra is a liquid crystal polymer thermoplastic that can be remelted and potentially used again. Two different carbon fillers (synthetic graphite particles and carbon fibers) were studied. Composites containing varying amounts of a single type of carbon filler were fabricated and tested. In addition, composites containing combinations of the synthetic graphite particles and carbon fibers were also investigated. The goal of this project was to determine how various amounts of the different carbon fillers affected the composite in-plane and through-plane thermal conductivity and to develop thermal conductivity models for the single filler and multiple filler systems.

Correspondence to: J. M. Keith (jmkeith@mtu.edu).

Contract grant sponsor: National Science Foundation; contract grant number: DMI-0456537.
Contract grant sponsor: Department of Energy; contract grant number: DE-FG02-04ER63821.

MATERIALS AND EXPERIMENTAL METHODS

Materials

The matrix material used in this study was Ticona's (Summit, NJ) Vectra A950RX liquid crystal polymer

TABLE I
Properties of Ticona's Vectra A950RX[19]

Melting point	280°C
Tensile modulus (1 mm/min)	10.6 GPa
Tensile strength at break (5 mm/min)	182 MPa
Tensile strain at break (5 mm/min)	3.4%
Flexural modulus at 23°C	9.1 GPa
Notched Izod impact strength at 23°C	95 kJ/m^2
Density at 23°C	1.40 g/cm^3
Volumetric electrical resistivity at 23°C	10^{15} Ω cm
Surface electrical resistivity	10^{14} Ω
Thermal conductivity at 23°C	0.22 W/m K (approx.)
Humidity absorption (23°C/50%RH)	0.03 wt %
Mold shrinkage-parallel	0.0%
Mold shrinkage-normal	0.7%
Coefficient of linear thermal expansion-parallel	0.04×10^{-4}/°C
Coefficient of linear thermal expansion-normal	0.38×10^{-4}/°C

(LCP). Vectra is a highly ordered thermoplastic copolymer consisting of 73 mol % hydroxybenzoic acid (HBA) and 27 mol % hydroxynapthoic acid (HNA). This LCP has the properties needed for bipolar plates, namely high dimensional stability up to a temperature of 250°C, short molding times (often 5–10 s), exceptional dimensional reproducibility, chemical resistance in acidic environments present in fuel cells, and a low hydrogen gas permeation rate.[19,20] The properties of this polymer are shown in Table I.[19]

Table II shows the properties of Asbury Carbons' (Asbury, NJ) Thermocarb TC-300, which is a synthetic graphite that was previously sold by Conoco

TABLE II
Properties of Thermocarb TC-300 Synthetic Graphite[21,22]

Carbon Content, wt %	99.91
Ash, wt %	<0.1
Sulfur, wt %	0.004
Density, g/cc	2.24
BET Surface Area, m^2/g	1.4
Thermal Conductivity at 23°C, W/m K	600 in "a" crystallographic direction
Electrical resistivity of bulk carbon powder at 150 psi, 23°C, parallel to pressing axis, Ω-cm	0.020
Particle shape	Acicular
Particle aspect ratio	1.7
Sieve analysis (μm)	wt %
+600	0.19
+ 500	0.36
+300	5.24
+ 212	12.04
+180	8.25
+150	12.44
+75	34.89
+44	16.17
−44	10.42

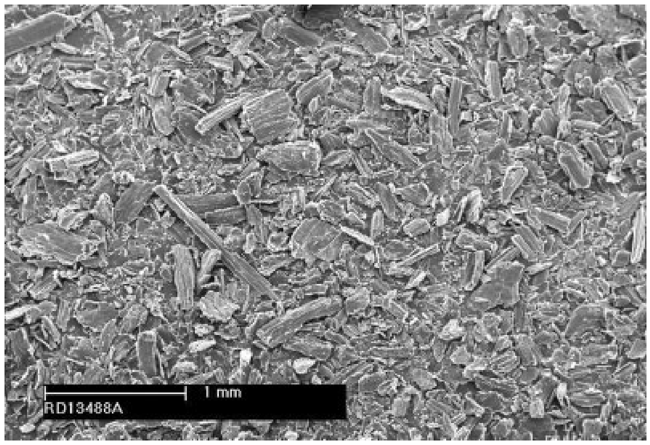

Figure 1 Photomicrograph of Thermocarb TC-300 synthetic graphite (Courtesy of Asbury Carbons).

(Houston, TX).[21,22] Thermocarb TC-300 is produced from a thermally treated, highly aromatic petroleum feedstock and contains very few impurities. Figure 1 shows a photomicrograph of this synthetic graphite.

Fortafil 243 carbon fiber, sold by Toho Tenax America (Rockwood, TN), was the second filler used in this study. Fortafil 243 is a polyacrylonitrile (PAN) based 3.2 mm chopped and pelletized carbon fiber that is often used to improve the electrical and thermal conductivity and the tensile strength of the resin. Fortafil 243 was surface treated and then formed into pellets by the manufacturer. A proprietary polymer (sizing) is used as a binder for the pellets that also promotes adhesion with the matrix. Table III shows the properties of this carbon fiber.[23]

The concentrations (shown in wt % and the corresponding vol %) for the single filler composites tested in this research are shown in Table IV. Increasing filler amount increases composite melt viscosity. The maximum single filler amounts that could be extruded and injection molded were 80 wt % (71.4 vol %) for synthetic graphite and 60 wt % (54.7 vol %) for carbon fiber. Table V shows the multiple filler

TABLE III
Properties of Fortafil 243 Carbon Fiber[23]

Carbon content	95 wt %
Electrical resistivity	0.00167 Ω-cm
Thermal conductivity	20. W/m K (axial direction)
Tensile strength	3800 MPa
Tensile modulus	227 GPa
Specific gravity	1.74 g/cc
Fiber diameter	7.3 μms
Fiber shape	Round
Fiber mean length	3.2 mm (entire range is 2.3 mm to 4.1mm)
Binder content	2.6 wt % proprietary polymer that adheres pellet together and promotes adhesion with nylon matrix
Bulk density	356 g/L

TABLE IV
Single Filler Loading Levels

Filler (wt %)	Thermocarb (vol %)	Fortafil (vol %)
5.0	N/A	4.1
7.5	N/A	6.1
10.0	6.5	8.2
15.0	9.9	12.4
20.0	13.5	16.8
25.0	17.2	21.2
30.0	21.1	25.5
35.0	25.2	30.2
40.0	29.3	34.9
45.0	33.8	39.7
50.0	38.5	44.6
55.0	43.3	49.6
60.0	48.4	54.7
65.0	53.7	N/A
70.0	59.3	N/A
75.0	65.2	N/A
80.0	71.4	N/A

formulations containing varying concentrations of the synthetic graphite particles and carbon fibers. Because this project focuses on producing highly conductive composites, loading levels were chosen so that the filler amounts would produce conductive composites, while still allowing the composite material to have a sufficiently low enough viscosity to be extruded and injection molded into test specimens.

Test specimen fabrication

For this entire project, the fillers were used as they were received. Vectra A950RX was dried in an indirectly heated dehumidifying drying oven at 150°C and then stored in moisture barrier bags.

The extruder used was an American Leistritz Extruder Corp. (Somerville, NJ) model ZSE 27. This extruder has a 27 mm corotating intermeshing twin screw with 10 zones and a length/diameter ratio of 40. The screw design, which is shown elsewhere,[24] was chosen to achieve a minimum amount of filler degradation, while still allowing the fillers to be well dispersed into the polymer. The polymer pellets (Vectra) were introduced in Zone 1. For the composites containing single fillers, the fillers were added into the polymer melt at Zone 5. For the composites containing combinations of fillers, carbon fiber was added into the polymer melt at Zone 7 and synthetic graphite was added to the polymer melt at Zone 5. Because of the large amounts of fillers added, to obtain good mixing it was not possible to add the fillers at the same zone. Schenck (Whitewater, WI) AccuRate gravimetric feeders were used to accurately control the amount of each material added to the extruder.

After passing through the extruder, the polymer strands (3 mm in diameter) entered a water bath and then a pelletizer that produced nominally 3-mm long pellets. After compounding, the pelletized composite resin was dried and then stored in moisture barrier bags before injection molding.

A Niigata (Itasca, IL) injection molding machine, model $NE85UA_4$, was used to produce test specimens. This machine has a 40 mm diameter single screw with a length/diameter ratio of 18. The lengths of the feed, compression, and metering sections of the single screw are 396, 180, and 144 mm, respectively. A mold was used to produce 3.2 mm thick, 6.4 cm diameter disks (end gated). Before conducting the thermal conductivity tests, the samples were conditioned at 23°C and 50% relative humidity for 88 h.[25]

Filler length, aspect ratio, and orientation test method

To determine the length and aspect ratio of the carbon fiber and synthetic graphite in the test

TABLE V
Multiple Filler Loading Levels and Thermal Conductivity Data

Formulation	Thermocarb wt % (vol %)	Fortafil wt % (vol %)	TCA-300 through-plane thermal conductivity (W/m K) at 55°C	Hot disk through-plane thermal conductivity (W/m K) at 23°C	Hot disk in-plane thermal conductivity (W/m K) at 23°C
1	40 (30.1)	10 (9.7)	1.200 ± 0.020 $n = 6$	1.193 ± 0.007 $n = 5$	5.758 ± 0.041 $n = 5$
2	40 (30.5)	15 (14.7)	1.483 ± 0.027 $n = 5$	1.479 ± 0.008 $n = 5$	6.461 ± 0.035 $n = 5$
3	40 (30.8)	20 (19.8)	1.960 ± 0.075 $n = 5$	1.956 ± 0.014 $n = 5$	7.521 ± 0.080 $n = 5$
4	50 (39.4)	10 (10.1)	2.130 ± 0.081 $n = 7$	2.120 ± 0.007 $n = 5$	9.629 ± 0.046 $n = 5$
5	50 (39.9)	15 (15.4)	2.806 ± 0.087 $n = 6$	2.807 ± 0.013 $n = 5$	12.01 ± 0.203 $n = 5$
6	60 (49.6)	10 (10.7)	4.298 ± 0.027 $n = 4$	4.333 ± 0.019 $n = 5$	17.49 ± 0.383 $n = 5$
7	65 (54.4)	5 (5.4)	4.553 ± 0.081 $n = 4$	4.572 ± 0.042 $n = 5$	16.81 ± 0.186 $n = 5$

specimens, diethylenetriamine was used to dissolve the matrix. The fillers were then dispersed onto a glass slide and viewed using an Olympus (Center Valley, PA) SZH10 optical microscope with an Optronics Engineering LX-750 video camera. Images of the filler were collected using Scion Image version 1.62 software. The length and aspect ratio of the fillers were measured using Adobe (San Jose, CA) Photoshop 5.0 and the Image Processing Tool Kit version 3.0. Additional details of this test method are shown elsewhere.[26,27]

To determine the orientation of the carbon fillers, a polished composite sample was viewed using an optical microscope. For the through-plane thermal conductivity samples, the center portion was cut out of a 6.4 cm diameter, 3.2 mm thick injection molded disk and then mounted in epoxy so that the through the sample thickness face could be viewed. For the in-plane thermal conductivity samples, the center portion was cut out of an injection molded tensile bar and the samples were cast in epoxy so that the direction of flow induced during the injection molding process, which was also the in-plane thermal conductivity measurement direction, would be viewed. The samples were then polished and viewed using an Olympus BX60 reflected light microscope. Again, the images were collected as described in the above paragraph. More details of this test method are shown elsewhere.[26,27]

Thermal conductivity: Guarded heat flow meter test method

The through-plane thermal conductivity of a 3.2 mm thick, 5 cm diameter disk shaped test specimen was measured at 55°C (as close to ambient temperature as can be measured while still maintaining a temperature gradient in the apparatus) using a Holometrix (Burlington, MA) Model TCA-300 Thermal Conductivity Analyzer, according to the ASTM F433 guarded heat flow meter method.[28] For each formulation, at least four samples were tested.

Thermal conductivity: Transient plane source technique

The Hot Disk Thermal Constants Analyzer, from Hot Disk (Piscataway, NJ), is an emerging technology that can measure the in-plane and through-plane thermal conductivity of an anisotropic material in the same test, using the transient plane source technique.[29–33] The sensor used in this test method consisted of a 10-μm thick nickel foil embedded between two 25.4-μm thick layers of Kapton polyimide film. The nickel foil was wound in a double spiral pattern and had a radius, R of either 3.189 mm or 6.403 mm. The thermal conductivities were measured at 23°C. Since our composites are anisotropic, this test method is useful for this project.

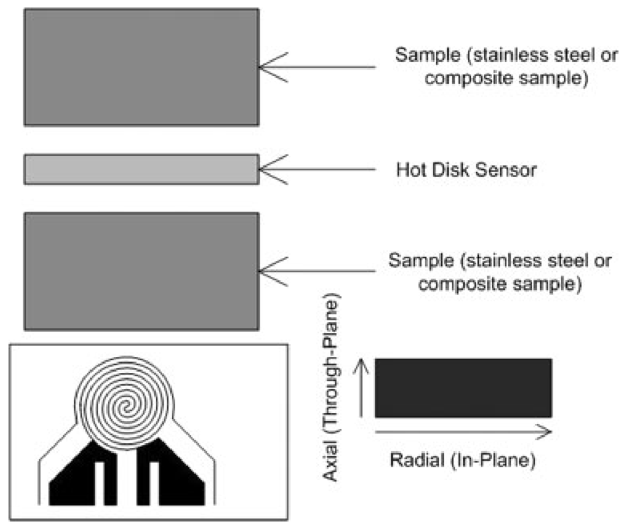

Figure 2 Schematic of samples and sensor for hot disk. The insert at the lower left shows the double spiral heating element.

Figure 2 shows how the sensor is positioned between two samples of composite material. In this experiment, the samples tested were composite disks of diameter $D = 6.4$ cm and thickness $x = 3.2$ mm. To help ensure that the assumption of an infinite sample domain was met and that heat was not penetrating completely through the sample in the axial direction, two of these composite disks were stacked together above the sensor and two more stacked below it, giving us a double thickness of sample. This stacking of disks allowed the generation of more reproducible data. For each formulation, typically five different sets of four disks (so a total of 20 disks) were tested.

The sensor then had a constant electrical current (variable by sample from 0.03 to 1.25 W) over a short period of time (variable by sample from 2.5 to 40 s) passed through it. The generated heat dissipated within the double spiral was conducted through the Kapton insulating layer and into the surrounding sample, causing a rise in the temperature of the sensor and the sample.

From a theoretical standpoint, the double spiral pattern can be approximated to a series of concentric, equally spaced ring sources. The characteristic heat conduction equation, assuming radial symmetry in the sample, is then given as[29–33]

$$(\rho C_p)\frac{\partial T}{\partial t} = k_{\mathrm{in}}\frac{1}{r}\left(\frac{\partial}{\partial r}\left(r\frac{\partial T}{\partial r}\right)\right) + k_{\mathrm{thru}}\frac{\partial^2 T}{\partial z^2} + \sum_{\mathrm{rings}} Q_r \delta(r - r')\delta(z) \quad (1)$$

where ρ is the density of the sample (kg/m^3), C_p is the heat capacity of the sample (J/(kg K)), T is the temperature of the sample (K), t is the time of the measurement (s), k_{in} and k_{thru} are the in-plane and through-plane thermal conductivities of the sample (W/m K), δ is the Dirac delta function, r' is the radius of one of the ring sources, and Q_r is the power supplied to that ring per unit length of the ring (W/m). The total power for each ring is proportional to the circumference of the ring $2\pi r'$, such that the total power supplied for all of the rings is Q (W). This total power Q is an input parameter to the Hot Disk Thermal Constants Analyzer. The first term in eq. (1) represents accumulation of thermal energy, the second term radial (referred to as in-plane in our experiments) heat conduction, the third term axial (referred to as through-plane in our experiments) heat conduction, and the final term is a heat source.

The sample can be approximated as an infinite domain if the experimental time is much less than the characteristic thermal diffusion time. For an anisotropic material in a cylindrical geometry, the experimental time must meet the following two criteria: $t \ll (D/2)^2/(\alpha_{\text{in}})$ and $t \ll x^2/(\alpha_{\text{thru}})$. In these formulas $\alpha = k/(\rho C_p)$ is the thermal diffusivity of the composite material.

The average transient temperature increase of the sensor is simultaneously measured by recording the change in electrical resistance of the nickel sensor[29–33] according to

$$\Delta T = \frac{1}{\beta}\left(\frac{R_n}{R_{\text{no}}} - 1\right) \tag{2}$$

where: ΔT is the change in temperature at time t (K), β is the temperature coefficient of resistance (TCR) of the material (1/K), R_n is the electrical resistance of the nickel at time t (Ω), and R_{no} is the electrical resistance of the nickel at time 0 (Ω). The temperature rise in eq. (2) is correlated with the in-plane and through-plane thermal conductivities through the solution of eq. (1) as

$$\Delta T = \frac{P}{\pi^{3/2} R \sqrt{k_{\text{in}} k_{\text{thru}}}} F(\tau) \tag{3}$$

where $F(\tau)$ is a dimensionless time dependent function of $\tau = \sqrt{\alpha_{\text{in}} t / R^2}$ given by an integral of a double series over the number of rings m

$$F(\tau) = [m(m+1)]^{-2} \times \int_0^{\tau} \sigma^{-2} \left[\sum_{l=1}^{m} l \sum_{k=1}^{m} k \exp\left(-\frac{l^2 + k^2}{4m^2\sigma^2}\right) I_0\left(\frac{lk}{2m^2\sigma^2}\right) \right] d\sigma \tag{4}$$

where σ is a variable of integration and l is the ring number. A more detailed derivation of eqs. (3) and (4) is given by He.[34] Equations (1) through (4) are used to determine the in-plane and through-plane thermal conductivity of the composite being tested.

RESULTS

Filler length, aspect ratio, and orientation results

The length and aspect ratio of the synthetic graphite in the injection molded composite samples was typically 50 μm and 1.68, respectively. These values are similar to the as received material and those obtained in prior work.[27,35] For the injection molded composites containing Fortafil 243, the length was typically 70 μm and the corresponding fiber aspect ratio (length/diameter) was 9. These results agree with prior work.[26,27,35,36]

The synthetic graphite particles and the carbon fibers in the in-plane thermal conductivity samples are primarily oriented in the in-plane thermal conductivity measurement direction, which was induced by the injection molding process. The fillers in the through-plane thermal conductivity samples are primarily oriented transverse to the thermal conductivity measurement direction. These observations agree with prior work and photomicrographs can be seen elsewhere.[26,27,35–38]

Through-plane thermal conductivity experimental results

Single filler formulations

The factors that affect the thermal conductivity of a composite are the filler size, shape, concentration, dispersion (degree of mixing), orientation, bonding between the filler and matrix, thermal conductivity of the constituents (filler and matrix), and the crystallinity of the polymer (increasing crystallinity improves thermal conductivity). Figures 3 and 4 show the experimental mean through-plane thermal conductivity as a function of filler volume fraction for composites containing Thermocarb and Fortafil 243, respectively. These formulations correspond to those shown in Table IV. The standard deviation was typically less than 5% of the mean.

The composites containing Thermocarb had the largest through-plane thermal conductivity values. At the highest filler level (80 wt % = 71.4 vol % synthetic graphite particles), the composite through-plane thermal conductivity increases from 0.22 W/m K (neat Vectra) to 10.1 W/m K. For the composites containing Fortafil 243, the through-plane thermal conductivity was 1.04 W/m K at the highest loading level (60 wt % = 54.7 vol %). Composites containing synthetic graphite likely had a higher through-plane thermal conductivity, compared with those containing carbon fiber, due to the higher thermal conductivity of the synthetic graphite particles (600 W/m K) versus the carbon fibers (20 W/m K).

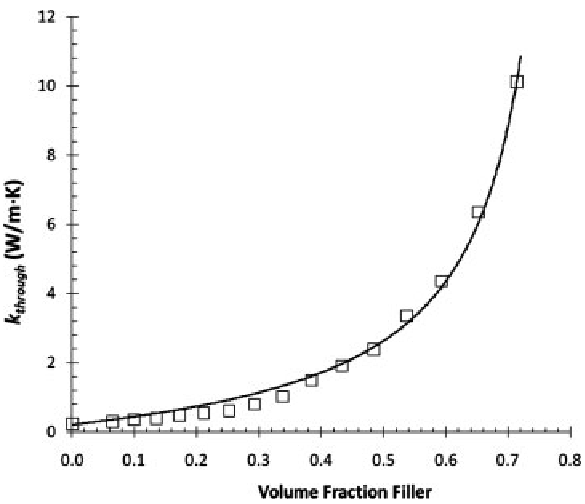

Figure 3 Experimental (squares) and theoretical (line) through-plane thermal conductivities for thermocarb TC-300 synthetic graphite/Vectra composites.

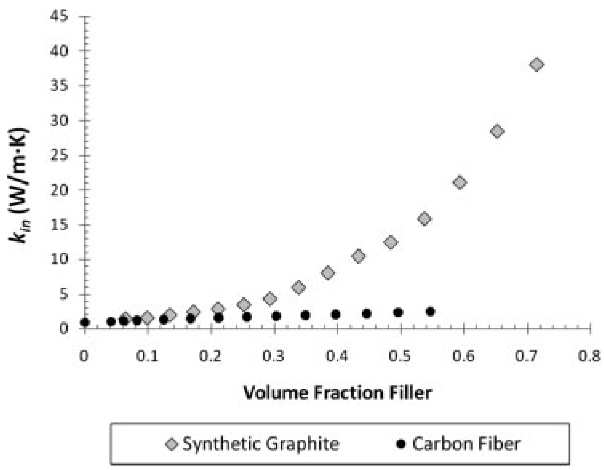

Figure 5 Experimental in-plane thermal conductivity for thermocarb TC-300 synthetic graphite/Vectra composites and Fortafil 243 carbon fiber/Vectra composites.

Multiple filler formulations

The mean through-plane thermal conductivity results, including the standard deviation and number of samples tested, for composites containing both Thermocarb and Fortafil 243 in varying concentrations are shown in Table V. The through-plane thermal conductivities range from 1.2 W/m K for Formulation 1 (40 wt % Thermocarb and 10 wt % Fortafil 243) to 4.6 W/m K for Formulation 7 (65 wt % Thermocarb and 5 wt % Fortafil 243).

In-plane thermal conductivity experimental results

Single filler formulations

Figure 5 shows the mean in-plane thermal conductivity as a function of filler volume fraction for composites containing only varying amounts of single fillers. These formulations correspond to those shown in Table IV. The standard deviation was typically less than 5% of the mean. In all cases, due to the flow patterns induced during the injection molding process and the anisotropy of the constituents, the composite in-plane thermal conductivity is higher than the through-plane thermal conductivity.

Figure 5 shows that the Thermocarb TC-300 synthetic graphite causes a larger increase in in-plane thermal conductivity. The value increases from 0.99 W/m K, which is the in-plane thermal conductivity of the polymer (anisotropic polymer so thermal conductivity is different in through-plane and in-plane directions), to 38 W/m K for composites containing 80 wt % (71.4 vol %) synthetic graphite. For the composites containing Fortafil 243, the in-plane thermal conductivity was 2.5 W/m K at the highest loading level (60 wt % = 54.7 vol %).

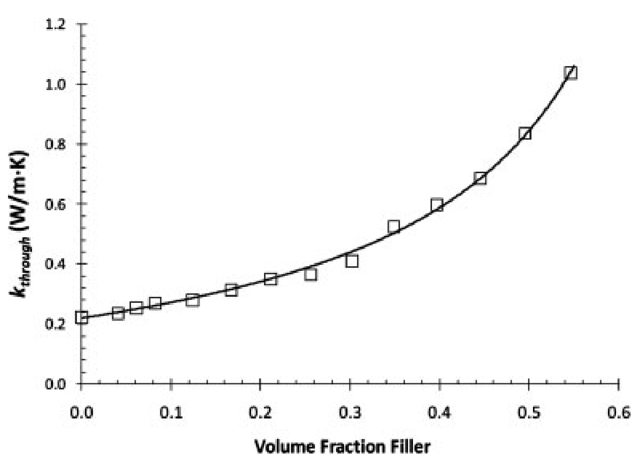

Figure 4 Experimental (squares) and theoretical (line) through-plane thermal conductivities for Fortafil 243 carbon fiber/Vectra composites.

Multiple filler formulations

The mean in-plane thermal conductivity results, including the standard deviation and number of samples tested, for composites containing both Thermocarb and Fortafil 243 in varying concentrations are shown in Table V. The through-plane thermal conductivity results from the transient plane source method at 23°C were approximately the same as the results obtained from the guarded heat flow meter method at 55°C. The in-plane thermal conductivities range from 5.8 W/m K for Formulation 1 (40 wt % Thermocarb and 10 wt % Fortafil 243) to 17 W/m K for Formulation 6 (60 wt % Thermocarb and 10 wt % Fortafil 243), and Formulation 7 (65 wt % Thermocarb and 5 wt % Fortafil 243).

Through-plane thermal conductivity modeling results

Single filler formulations

Thermal conductivity models can be used to predict the thermal conductivity of composites containing conductive fillers. Nielsen's model is the most versatile for conductive short fiber/particulate composites and accounts for constituent thermal conductivities, concentrations of each constituent, aspect ratio, orientation, and packing of the fillers.[36,39–41] The following equations were used to predict the through-plane thermal conductivity k_{through} (W/m K) of the conductive resins involved in this study

$$k_{\text{through}} = k_1 \frac{(1 + AB\phi)}{(1 - B\psi\phi)} \tag{5}$$

$$B = \frac{\left(\frac{k_2}{k_1} - 1\right)}{\left(\frac{k_2}{k_1} + A\right)} \tag{6}$$

In these equations, k_1 (W/m K) is the thermal conductivity of the polymer, k_2 (W/m K) is the thermal conductivity of the filler, ϕ is the filler volume fraction, A is a shape and orientation factor, and B is a factor that takes into account the relative conductivity of the two components. Finally, the ψ parameter, which is related to the 'maximum packing fraction', ϕ_m and the filler and polymer volume fractions, is given by Nielsen[40] as

$$\psi \cong 1 + \frac{1 - \phi_m}{\phi_m^2}\phi \tag{7}$$

To quantitatively show how the model compares to the experimental data, a standardized lack of fit term, ε was calculated using eq. (8).

$$\varepsilon = \frac{\sum_{i=1}^{n}(y_i - y_{\text{model}_i})^2}{\sum_{i=1}^{n} y_i^2} \tag{8}$$

In the above equation, y_i is the experimental thermal conductivity result, y_{model} is the thermal conductivity result predicted by the model, and i is the summation over all of the different formulations. A value of $\varepsilon = 0$ would indicate a perfect fit of the experimental data with the model.

Nielsen's model typically uses fixed data for the parameters A and ϕ_m, which are dependent on the filler shape, aspect ratio, and packing. Tables showing these parameters are given elsewhere.[36,39,40] However, these models have been shown to either underestimate the thermal conductivity or break down at high filler concentrations.[36,39,42,43] Thus, the theoretical through-plane thermal conductivities for Thermocarb and Fortafil 243 composites were calculated using eqs. (5)–(7) by adjusting the values for the shape factor A and the maximum packing fraction ϕ_m. For the composites containing Thermocarb TC-300 synthetic graphite, $k_2 = 600$ W/m K (Table II) and for the composites containing Fortafil 243 carbon fiber $k_2 = 20$ W/m K (Table III). In all cases, $k_1 = 0.22$ W/m K (Table I). The results are given as

Thermocarb: $A = 8.5$, $\phi_m = 0.82$, $\varepsilon = 3.4 \times 10^{-3}$

Fortafil 243: $A = 1.2$, $\phi_m = 0.76$, $\varepsilon = 7.1 \times 10^{-4}$

For each model, the A parameter was constrained to ensure that it was greater than zero. The A parameter values that were determined for each system can be attributed to the packing of the filler at high loading levels. The ϕ_m values were also constrained with the lower limit being the volume fraction of the composite containing the most filler (0.714 for Thermocarb and 0.547 for Fortafil) and the upper limit being the volume fraction of a composite that was not more than 10 wt % higher (0.85 for Thermocarb and 0.763 for Fortafil). Figure 3 shows how the model results compare to the experimental data for the composites containing Thermocarb and Figure 4 shows how the model results compare to the experimental data for the composites containing Fortafil. In both cases the model shows good agreement with the experimental data.

Multiple filler formulations

In this study, it was also desired to model the through-plane thermal conductivity of conductive resins that contained more than one conductive filler. A variation of eqs. (5)–(7) were used and are shown below.[36]

$$k_{\text{through}} = k_1 \frac{\left(1 + \sum_{i=2}^{n} A_i B_i \phi_i\right)}{\left(1 - \sum_{i=2}^{n} B_i \psi_i \phi_i\right)} \tag{9}$$

$$B_i = \frac{\left(\frac{k_i}{k_1} - 1\right)}{\left(\frac{k_i}{k_1} + A_i\right)} \tag{10}$$

$$\psi_i \cong 1 + \frac{1 - \phi_{\text{mi}}}{\phi_{\text{mi}}^2}\phi_i \tag{11}$$

In these equations, k_1 (W/m K) is the thermal conductivity of the polymer, k_i (W/m K) is the thermal conductivity of filler i, ϕ_i is the volume fraction of filler i, ϕ_{mi} is the maximum packing fraction of filler

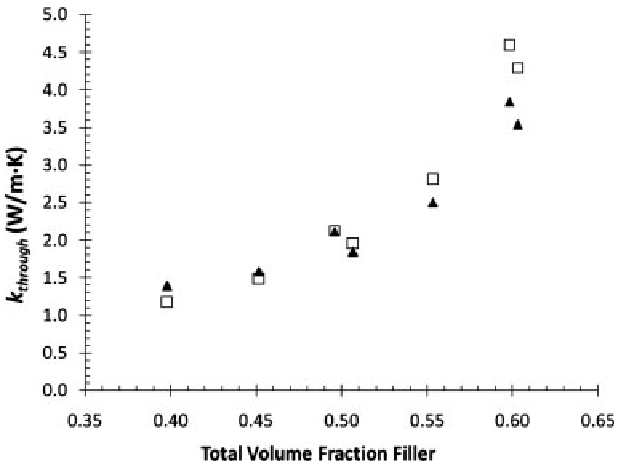

Figure 6 Experimental (squares) and theoretical (triangles) through-plane thermal conductivities for multiple filler formulations.

i, and A_i is a shape and orientation factor for each filler i. Since A_i and ϕ_{mi} are chosen depending on the filler(s) used in a formulation, there will be a separate B term and ψ term calculated for each filler.

The individual A and ϕ_m values that were obtained for the single filler through-plane thermal conductivity models for Thermocarb and Fortafil (mentioned above) were used in eqs. (9)–(11) to determine the theoretical through-plane thermal conductivities for composites containing combinations of Thermocarb and Fortafil 243. The results for these multiple filler formulations are shown in Figure 6, where the squares represent the experimental data and the triangles represent the theoretical through-plane thermal conductivities calculated using the model, and for this multiple filler model $\varepsilon = 0.022$. This multiple filler model shows good agreement with the experimental data without any further optimization of the A and ϕ_m parameters.

In-plane thermal conductivity modeling results

Single filler formulations

Using the in-plane and through-plane thermal conductivity results shown for the Thermocarb TC-300/Vectra A950RX composites in Figures 3 and 5, an exponential correlation between the square root of the product of the in-plane and through-plane thermal conductivities and the volume fraction filler was observed. This correlation is given by

$$\sqrt{k_{\text{in}} k_{\text{through}}} = 0.425 e^{5.272\phi} \quad \varepsilon = 1.4 \times 10^{-3} \qquad (12)$$

where k_{in} and k_{through} are the in-plane and through-plane thermal conductivity, respectively, and have units of (W/m K) and ϕ is the filler volume fraction. Rearranging for k_{in} yields the following predictive equation

$$k_{\text{in}} = \frac{\left(0.425 e^{5.272\phi}\right)^2}{k_{\text{through}}} = \frac{0.1806 e^{10.544\phi}}{k_{\text{through}}} \qquad (12a)$$

Figure 7 shows the experimental data plotted along with the predicted results of the model. The reason for the exponential term appearing in this model is related to the range of filler volume fractions being modeled.

Using the results in Figures 4 and 5, a correlation was developed for the Vectra/Fortafil 243 carbon fiber composites as

$$\sqrt{k_{\text{in}} k_{\text{through}}} = 0.478 e^{2.123\phi} \quad \varepsilon = 6.2 \times 10^{-5} \qquad (13)$$

Rearranging for k_{in} yields the following predictive equation

$$k_{\text{in}} = \frac{0.2285 e^{4.246\phi}}{k_{\text{through}}} \qquad (13a)$$

Figure 8 shows the experimental data plotted along with the predicted results of the model.

The above models can be combined with through-plane thermal conductivity models from the literature to predict the in-plane thermal conductivity of a Vectra-based single filler composite containing either Thermocarb TC-300 synthetic graphite (up to 71 vol %) or Fortafil 243 carbon fiber (up to 55 vol %).

Multiple filler formulations

Using the in-plane and through-plane thermal conductivity results obtained from the Hot Disk and shown in Table V, for composites containing both

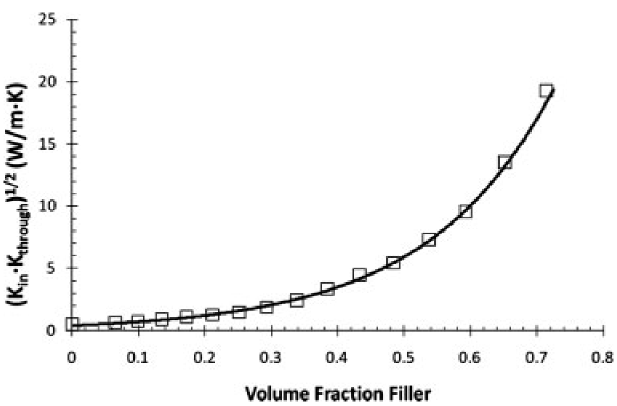

Figure 7 Square root of the product of in-plane and through-plane thermal conductivities for Thermocarb TC-300 synthetic graphite/Vectra composites. Data points are squares and a model fit is given by the solid line.

synthetic graphite and carbon fiber, an exponential correlation between the square root of the product of the in-plane and through-plane thermal conductivities and the volume fraction filler was observed. This correlation is given by

$$\sqrt{k_{\text{in}}k_{\text{through}}} = 0.452e^{5.272\phi_1+2.123\phi_2+1.128\phi_1\phi_2} \qquad \varepsilon = 5.9 \times 10^{-3} \tag{14}$$

where, k_{in} and k_{through} are the in-plane and through-plane thermal conductivity of the composite, respectively, ϕ_1 is the volume fraction of synthetic graphite and ϕ_2 is the volume fraction of carbon fiber. The term in front of the exponent in eq. (14) was determined by averaging the terms from the single filler models for the Thermocarb and Fortafil (shown above), which were 0.425 [eq. (12)] and 0.478 [eq. (13)], respectively. The first term in the exponent of eq. (14) was determined from the single filler model for the Thermocarb composites [eq. (12)] and the second term in the exponent was determined from the single filler model for the Fortafil 243 composites [eq. (13)]. The third term in the exponent is a nonlinear cross-term which accounts for interactions between the fillers and is the one unknown parameter in eq. (14), which was adjusted until the error term (ε) was as close to zero as possible.

Rearranging eq. (14) for k_{in} yields the following predictive equation:

$$k_{\text{in}} = \frac{0.2039e^{10.544\phi_1+4.246\phi_2+2.257\phi_1\phi_2}}{k_{\text{through}}} \tag{14a}$$

Figure 9 shows the experimental data plotted along with the predicted results of the model. This model can be combined with through-plane thermal con-

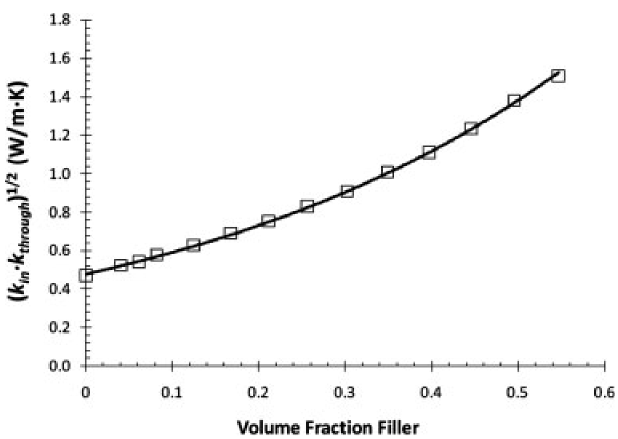

Figure 8 Square root of the product of in-plane and through-plane thermal conductivities for Fortafil 243 carbon fiber/Vectra composites. Data points are squares and a model fit is given by the solid line.

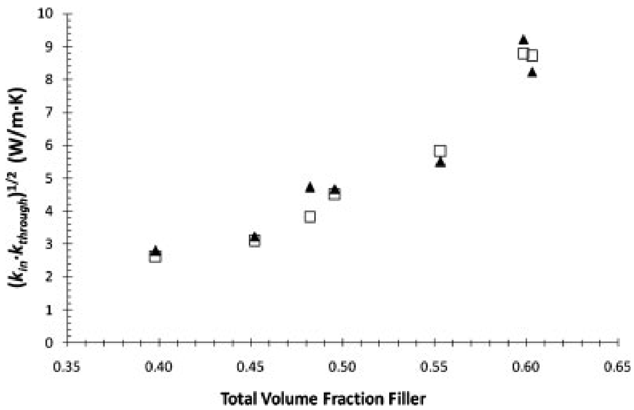

Figure 9 Square root of the product of in-plane and through-plane thermal conductivities for composites containing both Thermocarb TC-300 synthetic graphite and Fortafil 243 carbon fiber in Vectra. Experimental data points are squares and the theoretical model points are given by triangles.

ductivity models from the literature to predict the in-plane thermal conductivity of Vectra-based multiple filler conductive composites containing both Thermocarb TC-300 synthetic graphite and Fortafil 243 carbon fiber.

CONCLUSIONS

In this study, two different carbon fillers (Thermocarb synthetic graphite and Fortafil 243 carbon fiber) were added to Vectra A950RX LCP to produce single filler composites with filler concentrations of up to 80 wt % (71.4 vol %) and to produce multiple filler composites that contained both synthetic graphite and carbon fiber at varying concentrations. The in-plane and through-plane thermal conductivity for each formulation was measured. For the single filler formulations, those containing Thermocarb had higher in-plane and through-plane thermal conductivity, when compared to those containing Fortafil. Composites containing synthetic graphite likely had a higher thermal conductivity, compared with those containing carbon fiber, due to the higher thermal conductivity of the synthetic graphite particles (600 W/m K) versus the carbon fibers (20 W/m K).

Two through-plane thermal conductivity models and two models used to predict the in-plane thermal conductivity were the focus of this work. The Nielsen model was used to determine the theoretical through-plane thermal conductivity for the single filler Thermocarb and Fortafil formulations with the A and ϕ_m parameters optimized for each data set. A variation of the original Nielsen model was then used to accommodate for the formulations containing multiple fillers using the individual A and ϕ_m parameters that were previously determined for the single filler models. The single and multiple filler through-plane thermal conductivity models show good agreement with the experimental data.

The model that was used to predict the in-plane thermal conductivity of the single filler composites uses a correlation for the square root of the product of the experimental in-plane and through-plane thermal conductivities. A variation of this model and parameters obtained from the single filler in-plane thermal conductivity models were then used to predict the in-plane thermal conductivity of the composites containing both fillers. The in-plane thermal conductivity models for the single filler composites and the multiple filler formulations show good agreement with the experimental data.

The authors also thank the American Leistritz technical staff for recommending an extruder screw design and Asbury Carbons for providing the synthetic graphite.

References

1. Finan, J. M. Proceedings of the Society of Plastics Engineers Annual Technical Conference, New York, 1999, p 1547.
2. Agari, Y.; Uno, T. J Appl Polym Sci 1985, 30, 2225.
3. Bigg, D. M. Polym Eng Sci 1977, 17, 842.
4. Bigg, D. M. Polym Compos 1986, 7, 125.
5. Bigg, D. M. Polym Compos 1985, 6, 20.
6. Nagata, K.; Iwabuki, H.; Nigo, H. Compos Interfaces 1999, 6, 483.
7. Demain, A. Ph.D. Dissertation, Universite Catholique de Louvain, Louvain-la-Neuve, Belgium, 1994.
8. King, J. A.; Tucker, K. W.; Meyers, J. D.; Weber, E. H.; Clingerman, M. L.; Ambrosius, K. R. Polym Compos 2001, 22, 142.
9. Murthy, M. V. Proceedings of the Society of Plastics Engineers Annual Technical Conference, San Francisco, CA, 1994, p 1396.
10. Simon, R. M. Polym News 1985, 11, 102.
11. Mapleston, P. Mod Plast 1992, 69, 80.
12. Donnet, J.-B.; Bansal, R. C.; Wang, M.-J. Carbon Black; 2nd ed.; NY: Marcel Dekker Inc, 1993.
13. Huang, J.-C. Adv Polym Tech 2002, 21, 299.
14. Bigg, D. M. Polym Eng Sci 1979, 19, 1188.
15. Wilson, M. S.; Busick, D. N. U.S. Pat. 6,248,467 (2001).
16. Loutfy, R. O.; Hecht, M. U.S. Pat. 6,511,766 (2003).
17. Braun, J. C.; Zabriskie, J. E., Jr.; Neutzler, J. K.; Fuchs, M.; Gustafson, R. C. U.S. Pat. 6,180,275 (2001).
18. Mehta, V.; Cooper, J. S. J Power Sources 2003, 114, 32.
19. Ticona Vectra Liquid Crystal Polymer (LCP) Product Information, Ticona, Summit, N.J.; 07901 (2000).
20. Chiou, J. S.; Paul, D. R. J Polym Sci Part B: Polym Phys 1987, 25, 1699.
21. Asbury Carbons Product Information, Asbury, N. J.; 08802 (2004).
22. Conoco Carbons Products Literature, Conoco, Inc. P. O. Box 2197, Houston, T. X.; 77252–2197 (1999).
23. Toho Tenax America, Inc. Fortafil Carbon Fibers Technical Data Sheet, 121 Cardiff Valley Road, Rockwood, TN 37854.
24. King, J. A.; Morrison, F. A.; Keith, J. M.; Miller, M. G.; Smith, R. C.; Cruz, M.; Neuhalfen, A. M.; Barton, R. L. J Appl Polym Sci 2006, 101, 2680.
25. ISO 291:1997. Plastics-standard atmospheres for conditioning and testing. ISO 291:1997, International Standard Organization, Switzerland (1998).
26. Heiser, J. A.; King, J. A. Polym Compos 2004, 25, 186.
27. Heiser, J. A.; King, J. A.; Konell, J. P.; Sutter, L. L. Polym Compos 2004, 25, 407.
28. ASTM. Evaluating thermal conductivity of gasket materials. ASTM Standard F433–77 (Reapproved 1993), American Society for Testing and Materials, Philadelphia (1996).
29. Gustavsson, M.; Karawacki, E.; Gustafsson, S. E. Rev Sci Instrum 1994, 65, 3856.
30. Log, T.; Gustafsson, S. E. Fire Mater 1995, 19, 43.
31. Bohac, V.; Gustavsson, M. K.; Kubicar, L.; Gustafsson, S. E. Rev Sci Instrum 2000, 71, 2452.
32. Mathis Instruments, Ltd. Hot Disk Thermal Constants Analyzer Instruction Manual, Mathis Instruments, Ltd., Fredericton, New Brunswick, Canada (2001).
33. National Physical Laboratory. Transient Plane Source-Gustafsson Hot Disk Technique, Standards for Contact Transient Measurements of Thermal Properties. National Physical Laboratory: United Kingdom, accessed February 2008 at http://www.npl.co.uk/thermal/ctm.
34. He, Y. Thermochimica Acta 2005, 436, 122.
35. Konell, J. P.; King, J. A.; Miskioglu, I. Polym Compos 2004, 25, 172.
36. Weber, E. H.; Clingerman, M. L.; King, J. A. J Appl Polym Sci 2003, 88, 123.
37. King, J. A.; Miller, M. G.; Barton, R. L.; Keith, J. M.; Hauser, R. A.; Peterson, K. R.; Sutter, L. L. J Appl Polym Sci 2006, 99, 1552.
38. Keith, J. M.; King, J. A.; Grant, P. W.; Cole, A. J.; Klett, B. M.; Miskioglu, I., Polym Compos 2008, 29, 15.
39. Weber, E. H. Ph.D. Dissertation, Michigan Technological University, Houghton, MI, 2001.
40. Nielsen, L. Ind Eng Chem Fundam 1974, 13, 17.
41. McGee, S.; McCullough, R.L. Polym Compos 1981, 2, 149.
42. King, J. A.; Tucker, K. W.; Vogt, B. D.; Weber, E. H.; Quan, C. Polym Compos 1999, 20, 643.
43. Miller, M. G. Ph.D. Dissertation, Michigan Technological University, Houghton, MI, 2006.